Proceedings World Geothermal Congress 2020+1
Reykjavik, Iceland, April - October 2021

Physical, Chemical and Mineralogical Evolution of the Tolhuaca Geothermal System, Southern Andes, Chile

Pablo Sanchez-Alfaro, Pamela Perez-Flores, Daniele Tardani, Martin Reich, José Cembrano, Julie Rowland and Gloria Arancibia

[1]Instituto Ciencias de la Tierra, Universidad Austral de Chile; [2]Andean Geothermal Centre of Excellence, Universidad de Chile; [3] Pontificia Universidad Católica de Chile

pablo.sanchez@uach.cl

Keywords: Tolhuaca geothermal system, fault-fracture networks, hydrothermal alteration, fluid inclusions, Liquiñe-Ofqui fault system.

ABSTRACT

The interplay between heat-fluid-rock interaction processes and brittle deformation is fundamental in the development of geothermal systems. However, the feedback mechanisms of such interplay and their effects on the duration and thermal structure of the geothermal system are poorly constrained. The work presented here address this issue by studying the physical, chemical and mineralogical evolution of the active Tolhuaca geothermal system in the Andes of southern Chile. We used temperature measurements in the deep wells and geochemical analyses of borehole fluid samples to constrain present-day fluid conditions. In addition, we used paleo-fluid temperatures and chemistry from microthermometry, and LA-ICP-MS analysis of fluid inclusions taken from well-constrained parageneses in vein samples retrieved from the Tol-1 borehole core. Complementarily, we investigate the effect that fluid chemistry changes can have on the zonation sulphides by using quantitative micro-analyses of pyrite at grain-scale of samples retrieved from Tol-1. We also analyse the effect of the development of a low-cohesion low-permeability clay cap on the long-term thermal structure of the system by using numerical simulations of heat and fluid flows. These chemical and mineralogical analyses are integrated with a structural study of the geometry and kinematics of the faults and fractures from the Tol-1 borehole.

Results show that hydrothermal alteration at Tolhuaca has produced structural and hydrological compartmentalisation of the system by developing an upper, low-permeability and low-cohesion clay-rich zone. In this zone, the formation of extensional fractures is inhibited, contributing to sustaining low-permeability conditions. Numerical simulations of heat and fluid flow support our observations and suggest that the presence of a low permeability clay-cap triplicates the duration of high enthalpy conditions in the deep upflow zone of Tolhuaca. These data reveal that the dynamic interplay between fluid flow, crack-seal processes and hydrothermal alteration are key factors in the evolution of the reservoir at the flank of the Tolhuaca volcano. Our results show that the favourability for developing geothermal resources in the southern Andes is highly dependent on such dynamic interplay.

1. INTRODUCTION

Geothermal systems have been largely understudied in the Andes, and in particular, there is limited scientific information on the origin and evolution of active hydrothermal systems (Sanchez-Alfaro et al., 2015). A better understanding of the mineralogical, chemical and structural evolution of Andean geothermal systems is key to develop efficient and environmentally friendly exploration strategies of energy resources with a regional focus (Moore and Simmons, 2013; Sanchez-Alfaro et al., 2015).

Since changes on the thermodynamic condition of hydrothermal systems strongly affect mineral stability, it is possible to track the long term temperature, pressure and fluid chemistry evolution of the system by analysing their mineral parageneses (e.g., Browne, 1978). Therefore, mineralogical studies may reveal the main processes occurring during the development of geothermal reservoirs, such as heating, cooling, fluid mixing, among others (Browne, 1978; Moore et al., 2008; Simmons and Browne, 2000). The active precipitation of hydrothermal minerals often produces crack sealing and loss of permeability that inhibits efficient fluid flow (Davatzes and Hickman, 2010). The opposite effect has fault-fracture networks activity that episodically produces an enhancement of permeability in brittle rocks (e.g. Davatzes and Hickman, 2010; Meller and Kohl, 2014). In particular, it has been shown that the reactivation of optimally oriented and critically stressed fractures is an important mechanism in maintaining high reservoir permeability in some geothermal systems by opening new and pre-existent fractures (Davatzes and Hickman, 2010; Hanano, 2004; Meller and Kohl, 2014). However, rocks with ductile behaviour such as hydrothermal clays, which are characterised by low permeability, commonly reduce the strength and the cohesion of the fractures (Dobson et al., 2003; Neuzil, 1994; Wyering et al., 2014). These conditions promote shear and inhibit dilatation of pre-existent fractures, and therefore it has been suggested that in rocks that are pervasively altered to clays, deformation is not an efficient mechanism to enhance permeability (Davatzes and Hickman, 2010; Dobson et al., 2003)

On a geothermal reservoir scale, the aforementioned processes lead to areas where brittle (e.g., quartz/calcite-filled) fracture networks correlate with enhanced fluid flow, while clay-bearing fault/fracture zones act as persistent barriers (Davatzes and Hickman, 2010; Meller and Kohl, 2014; Rowland and Sibson, 2004). Therefore, hydrothermal alteration and fault system activity compartmentalise geothermal systems and may both enhance or inhibit hydrothermal fluid flow (Davatzes and Hickman, 2010; Rowland and Simmons, 2012). Although such relevant studies have provided evidence that both permeability and mineralisation are strongly affected by processes associated with heat-fluid-rock interaction, a model that integrates the feedback mechanisms involved and their effect on the condition for fault rupture is currently lacking for geothermal reservoirs in the Andes. Furthermore, the effect in the duration and thermal structure of the hydrothermal system that such interaction may produce – and thus, the sustainability of the geothermal energy resource in the Andes – remains largely unconstrained.

An excellent natural laboratory to study the evolution of Andean hydrothermal systems is the Andean Cordillera of Central-Southern Chile, where the abundant geothermal resources have been recently explored, and thus, subsurface mineralogical, geochemical and geophysical data is accessible (Aravena et al., 2016; Lahsen et al., 2010). This region also offers the opportunity to explore the feedback between brittle deformation and heat-fluid-rock interaction because active hydrothermal systems occur in close spatial relationship with active volcanism as well as major seismically-active fault systems (Cembrano and Lara, 2009). In the southern Andes Volcanic Zone, between 39° and 46°S, the volcanic and hydrothermal activity is controlled by the NNE-trending, 1,200 km long Liquiñe-Ofqui Fault System (LOFS) and the NW-trending Andean Transverse Faults (ATF), which host ~25% of geothermal features in the Chilean Andes (Lahsen et al., 2010; Sánchez et al., 2013; Sanchez-Alfaro et al., 2015). Within this setting, the active Tolhuaca geothermal field in the northern termination of the LOFS (Fig. 1) has recorded the typical sequence of hydrothermal alteration of high enthalpy systems (Melosh et al., 2012). Furthermore, the Tolhuaca geothermal system is one of the very few systems that have been drilled by geothermal companies in the whole region, with an estimated power potential of 70 MWe (Aravena et al., 2016). The deep exploration drillings performed by MRP Geothermal Chile Ltda (formerly GGE Chile SpA) allows the investigation of a hydrothermal system not yet affected by geothermal production or re-injection (Melosh et al., 2012, 2010).

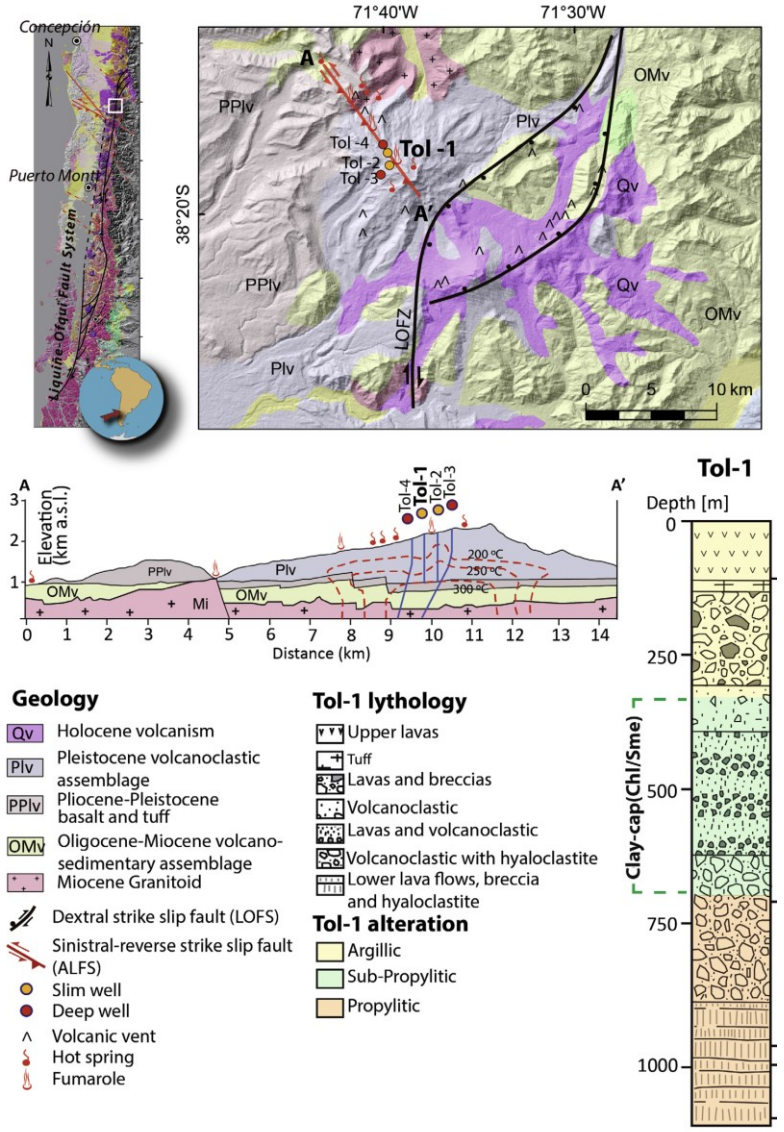

Figure 1: Geological map of the Tolhuaca Geothermal System from modified from Tardani et al., (2017), Aravena et al. (2016) and Sánchez-Alfaro et al. (2016a). The main geologic units, structures, surface thermal features and geothermal well locations, as well as the schematic cross-section, were modified from Sánchez-Alfaro et al. (2016a). Simplified lithology of the Tol-1 well and hydrothermal alteration zones were taken from Melosh et al. (2010; 2012) and Sánchez et al. (2013). LOFZ: Liquiñe Ofqui Fault Zone; ALFS: Arc-oblique Long-lived Basement Fault System.

The goal of this work is to present an integrated perspective of the physical, chemical and mineralogical evolution of the Tolhuaca geothermal system. To achieve this aim, we present the mineral paragenesis at Tolhuaca, obtained by using optical petrography and scanning electron microscopy (SEM) in veins and rock samples obtained from a deep (~1000 km) borehole core named Tol-1 (Sanchez-Alfaro et al., 2016). Tol-1 is a non-oriented, vertical borehole that recovered relatively young (>1 Ma) basaltic/andesitic volcanic rocks with subordinate pyroclastic/volcanoclastic interbedded units of Pleistocene age located in the NW-flank of the Tolhuaca volcano. In addition, temperature measurements in the deep wells and geochemical analyses of fluid samples retrieved from the reservoir were used to constrain present-day fluid conditions. We complemented this information by reconstructing the paleo-fluid temperature and chemistry from fluid inclusions microthermometry and LA-ICP-MS analyses of single fluid inclusions in

representative assemblages. We also analysed a comprehensive major and trace element database of pyrite obtained by using a combination of electron microprobe analysis (EMPA) and secondary ion mass spectrometry (SIMS) in a suite of well-constrained pyrite samples retrieved from Tol-1 (Tardani et al., 2017).

Furthermore, we complemented the geochemical analysis with structural information of the geometry, kinematics and mineralogical content of faults and veins recovered from Tol-1 borehole core. Since our results indicated the development of a low permeability clay cap, we simulate the impact of such a low permeability zone on the evolution of pressure and temperature conditions in the reservoir by using numerical simulations of heat and fluid flow. By integrating this data, our analysis constrains the optimal conditions leading to the development of high enthalpy geothermal resources in the Southern Andes.

2. THE TOLHUACA GEOTHERMAL SYSTEM

The Tolhuaca geothermal system is located in the northwest flank of the Tolhuaca volcano and is characterised by several surficial thermal manifestations including solfatara areas with fumaroles, boiling pools and hot springs (Fig. 1). Geothermal exploration campaigns comprising surface mapping, fluid geochemistry analyses, resistivity (MT) measurements and borehole logging have revealed the existence of a high enthalpy reservoir in the system (Melosh et al., 2012, 2010). Two slim holes (Tol-1 and Tol-2) and two larger diameter wells (Tol-3 and Tol-4) were drilled down to 2117 m vertical depth. Of the two slim holes, rock cores were retrieved during drilling only from Tol-1; it is important to emphasise that this is the only available diamond drilled core material at Tolhuaca that can be used to undertake a detailed mineralogical analysis of veins and fractures (in wells Tol-2, Tol-3 and Tol-4 only drill cutting samples were retrieved). Temperature logging and fluid samples suggest the presence of a geothermal reservoir at c.a. 1.5 km depth, at liquid-saturated conditions with temperatures up to 300°C and a relatively strong meteoric water component (Melosh et al., 2012). The main reservoir is overlain by a steam-heated aquifer at shallow depths that reaches up to 160°C and controls the nature of most of the hot springs (Melosh et al., 2012, 2010).

Rocks at Tolhuaca boreholes are mainly of basaltic andesite composition, although the whole-rock chemical range varies from basalt to dacites (Lohmar et al., 2012). Deposit types observed are mainly lavas and related breccias, volcaniclastics and minor tuffs. Hyaloclastites and pillow breccia occur at different levels in the Tol-1 core, indicating that lavas erupted during several time periods were in contact with glacial ice and/or water (Lohmar et al., 2012). Lohmar et al. (2012) suggest that the thick sequence dominated by volcaniclastic rocks in most of the bottom portions of the deepest wells (Tol-3 and Tol-4) may correspond to the Miocene Cura Mallín Formation (Niemeyer & Muñoz, 1983). In Tol-3 well, the Malleco and Cura Mallín formations are cut by numerous weakly altered, fine- to medium-grained intrusions that are interpreted as feeders to the Tolhuaca volcanic (Lohmar et al., 2012).

Surface hydrothermal alteration shows widespread acid-sulphate style mineralisation toward the summit of Tolhuaca Volcano. Argillic alteration is scattered at the surface in the main part of the geothermal prospect (Melosh et al., 2010). Based on thin section and XRD analyses of the Tol-1 core (Fig. 2), Melosh et al. (2012) defined an upper zone of argillic alteration (20 to 450 m), an intermediate zone with phyllic alteration (450 to 650 m), and a deeper zone of propylitic alteration (≥ 650 m). These authors characterised argillic alteration facies by Fe-oxides + chlorite + calcite + clay ± quartz ± pyrite, whereas high-temperature propylitic facies are composed of chlorite + epidote + calcite ± pyrite ± quartz ± zeolites mineral assemblages.

Borehole temperature and temperature gradient data from the deep wells indicate that hydrology and heat transfer regime is vertically segmented. The shallow level (0-300 m) presents a steep temperature gradient (< 150°C/km) and hosts a steam-heated aquifer with high vapour content between 100 and 200 m depth (Melosh et al., 2012). The inverse temperature gradient from two wells indicates lateral fluid flow and meteoric water infiltration. The intermediate level is characterised by a relatively constant, conductive-type gradient of 20-30°C/km occurring in most of the wells. At ~670 m, a transition towards an almost isothermal gradient of < 5°C/km, typical of convective heat transfer regimes, is observed (Fig. 3).

Subsurface resistivity data of the Tolhuaca geothermal system has been obtained from geophysical studies using magnetotelluric (MT) and audio frequency magnetotelluric soundings (AMT) methods (Melosh et al., 2012, 2010). Because the clay alteration that commonly caps geothermal reservoirs is low resistivity, MT and AMT are able to delineate such cap and, by association, the reservoir. Low resistivity at about 400 m depth occurs along the NW flank of the Tolhuaca volcano, following the trend of fumaroles and hot springs (Melosh et al., 2012, 2010). Another part of the resistivity anomaly extends to the south on the western flank of the stratovolcano. Argillic alteration mapped at the surface and in the wells confirms that argillic alteration is the primary cause of the low resistivity layer near the thermal areas (Melosh et al., 2012, 2010).

3. RESULTS

3.1 Mineral Paragenesis

Drill core logging and petrographic observations reveal that the Tolhuaca geothermal system is characterised by mineralogical and structural compartmentalisation (Figs. 1). Three hydrothermal alteration zones were recognised: (1) a shallow argillic alteration zone (0-300 m), characterised by clay minerals (smectite, interlayered chlorite-smectite), iron oxides and stilbite; (2) an intermediate sub-propylitic alteration zone (300-670 m), dominated by widespread and pervasive occurrence of interlayered chlorite-smectite and illite; and (3) a deep propylitic zone (670-1073 m), characterised by the occurrence of epidote and chlorite. The intensity of alteration in the groundmass and phenocrysts is variable, even at thin-section scale. However, the highest intensity is observed in the shallow region (~100 m depth) near the location of the steam-heated aquifer.

3.2 Fluid Inclusion Petrography, Microthermometry and Chemistry

Fluid inclusion petrography, microthermometry and LA-ICP-MS analyses were performed on in quartz and calcite crystals from eleven veins and fault veins from paragenetic stages S2, S3 and S4 comprising the three mineralogical segments. Only primary and pseudo-secondary fluid inclusions were chosen for analysis, although secondary fluid inclusion assemblages (FIAs) were measured but considered only for interpretations related to the latest alteration stage (S4).

The average total homogenization (Th_{tot}) and final ice melting (Tm_{ice}) temperatures for each FIAs are plotted as a function of depth in Figure 8. The temperatures of first ice melting were close to -23°C, strongly suggesting the presence of NaCl–H_2O-dominated fluids. All fluid inclusions show final ice melting in the temperature range between -0.0 and -2.3°C, corresponding to salinities that range from 0 to 3.8 wt.% eq. NaCl. The presence of substantial concentrations of CO_2 in the fluid inclusions is excluded because no clathrate melting was observed upon heating to room temperature. The microthermometric data show a correlation within ±40°C between Th and present-day temperatures measured in wells. The Th_{tot} data of FIAs related to the S3 stage indicate that the boiling temperature was reached, which is consistent with mineral textures such as lattice-bladed calcite. The Th_{tot} measured in FIAs related to the latest paragenetic stage (S4) are similar to present borehole temperatures.

The chemistry of fluid inclusions was quantified using LA-ICP-MS in fifteen out of near two hundred (206) of fluid inclusions analysed. Elements analysed were restricted to Cu, Zn, B and As due to the small amount of sample fluid (<10 ng) contained in the small (<80 µm) and low salinity (<3 wt.% eq. NaCl) fluid inclusions at Tolhuaca. To the best of our knowledge, these are the first quantitative chemical data of single fluid inclusions in an active geothermal system. The quantitative results on the fluid inclusion chemistry indicate that, after Na, B is the most abundant element. B/Na and As/Na molar ratios present a slight tendency to increase with time in the different paragenetic stages. Zn/Na and Cu/Na molar ratios were measured in one paragenetic stage, and therefore, their chemical evolution is possible to analyse only with respect to borehole fluids (Fig. 2). Variation with respect to depth of the elemental concentration ratios for the different FIAs identified are smaller than an order of magnitude and do not show a clear varying tendency.

3.3 Borehole Fluid Chemistry

The chemistry of borehole fluids at Tolhuaca was determined from aqueous samples retrieved from the Tol-4 deep geothermal well during a flow test. The main chemical features of the liquid phase are low salinity (Na=182 mg/kg; Cl=266 mg/kg) and sulphur contents (SO_4=8.7 mg/kg), and relatively high concentrations of metals including Au (1.57 µg/kg), Ag (0.018 µg/kg), Cu (0.07 µg/kg) and Zn (7.5 µg/kg). Boron (219 mg/kg) and As (25.6 mg/kg) contents are particularly high. In Figure 9 and Table 1, borehole fluid chemistry is compared with the quantitative measurements in fluid inclusions. These results show that fluid inclusions (paleofluids) and borehole (present-day) fluids at Tolhuaca are significantly different in terms of chemical composition. While borehole fluids are rich in Au, B and As, but Cu-poor (B/Na ~ $10^{0.5}$, As/Na ~ $10^{-1.1}$, Cu/Na ~ $10^{-4.2}$), the paleofluids trapped in fluid inclusions are Cu-rich but poor in B and As (B/Na ~ 10^{-1}, As/Na ~ $10^{-2.5}$, Cu/Na ~ $10^{-2.5}$ in average).

3.4 Pyrite

The concentrations of precious metals (e.g., Au, Ag), metalloids (e.g., As, Sb, Se, Te), and base and heavy metals (e.g., Cu, Co, Ni, Pb) in pyrite at Tolhuaca are significant. Among the elements analysed, As and Cu are the most abundant with concentrations that vary from sub-ppm levels to a few wt. % (i.e., up to ~5 wt. % As, ~1.5 wt. % Cu). Detailed wavelength-dispersive spectrometry (WDS) X-ray maps and secondary-ion mass spectrometry (SIMS) depth vs isotope concentration profiles reveal that pyrites from the TGS are characterised by chemical zoning. Well-developed zonations were detected in pyrite from the shallow argillic alteration zone, where, Cu(Co)-rich, As-depleted cores alternate with Cu(Co)-depleted, As-rich rims. These microanalytical data were contrasted with chemical data of fluid inclusions in quartz and calcite veins (high Cu/As ratios) and borehole fluid (low Cu/As ratios) reported at the Tolhuaca geothermal system, showing a clear correspondence between Cu and As concentrations in pyrite-forming fluids and chemical zonation in pyrite (Fig. 2).

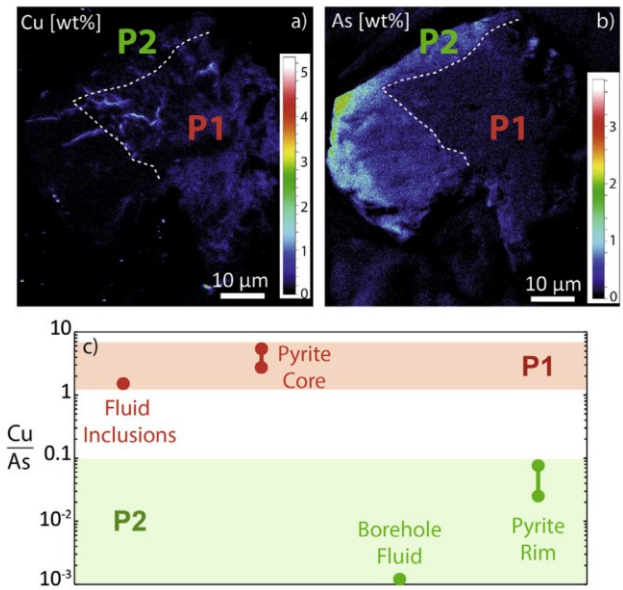

Figure 2: Combination of pyrite data (WDS X-ray maps) with LA-ICP-MS analyses of fluid inclusions in pyrite-bearing veins and borehole fluids chemical data at the Tolhuaca geothermal system, from Tardani et al., (2017). The panels (a) and (b) show a pyrite grain from the argillic zone that contains a Cu-rich, As-poor core (P1), and an As-rich, Cu-poor rim (P2). The panels (c) shows the Cu/As the ratio of fluid inclusions (red circles) and borehole fluids samples (green circles), respectively, reported by Sánchez-Alfaro et al. (2016). The Cu-rich, As-poor pyrite core (P1) correlates with the high Cu/As ratios measured in fluid inclusions in calcite-quartz-pyrite veins. Conversely, As-rich and Cu-poor pyrite rims (P2) correlate with the low Cu/As and ratio measured in the present-day borehole fluid.

3.5 Structural Elements on Tol-1 Borehole

The azimuthal orientation of fault and veins was determined after reorienting 66 pieces of Tol-1 using reliable remnant magnetisation vectors obtained by thermal (up to 700ºC on steps of 50°) demagnetisation methodology (Perez-Flores et al., 2016). Declination of RM vectors was used to re-orient the borehole pieces, as well as fault and veins, to a common anchor orientation consistent with the Geocentric Axial Dipole model given the young age of these rocks (Perez-Flores et al., 2016).

Detailed mapping of the Tol-1 borehole identifies 93 mesoscopic-scale veins and faults. Reoriented structures show a slight NE- and NW-striking preferential orientation. We recognised two major fault zones at 310 m and 660 m (with 50 cm and 40 cm of gouge, respectively); their precise orientation was not possible to obtain because of their irregular boundary. These fault zones are spatially associated with alteration zones boundaries. The reoriented structural elements show a wide distribution of strike and dip throughout the core. We recognised three zones with contrasting faults and veins patterns (strike and dip) and hydrothermal alteration mineral assemblages. There is a shallow (above 450 m depth) zone, where faults and veins are filled with one or more of the following minerals: Fe-oxides, calcite, quartz, silica, chalcedony, zeolite and chlorite/smectite. Mineral assemblages indicate an argillic alteration type. Breccia textures are typically found at the bottom of this structural zone. Faults and veins in the shallow zone display a wide range of strikes and dips. Faults and hybrid faults filled with calcite, quartz, chalcedony, chlorite/smectite and less common Fe-oxide, zeolite, silica and magnetite dominate the intermediate (400-700 m) zone indicating a sub-propylitic alteration type. Faults orientation predominantly are NNE-ENE-striking and >50° dipping. Finally, veins filled with epidote, calcite, zeolite, prehnite, quartz, pyrite and less common chalcedony and chlorite/smectite dominate the deep zone (>700 m); indicating a propylitic alteration type. Similar to the veins and hybrid faults observed up-hole, here, these structural elements are predominantly NNE-ENE-striking and >50° dipping. Veins show an EW- to NE- preferential orientation, with thicknesses that vary throughout the core between 1 to 20 mm.

3.5.1 Strain Field

Fault-slip data inversion yielded a widely scattered distribution for both P- and T-axes clusters. P-axes are roughly distributed along a major circle on an EW direction whereas T-axes are scattered about N and S orientations. The mean shortening vector is oriented 352º/38º (95 per cent confidence cone = 20°), and the stretching vector is 177º/78º (a95 = 19°).

3.5.2 Stress Field

The dynamic analysis shows a well-defined orientation for both clusters of σ_1 and σ_3 axes, with a normal-like distribution of Φ values (maximum value Φ=0.4). This analysis indicates a tensional tectonic regime with vertical σ_1 (083º/74º) and N-trending subhorizontal σ_3 (184°/03°). Small values of angular misfit indicate that nearly all of the analysed faults respond to a common stress field.

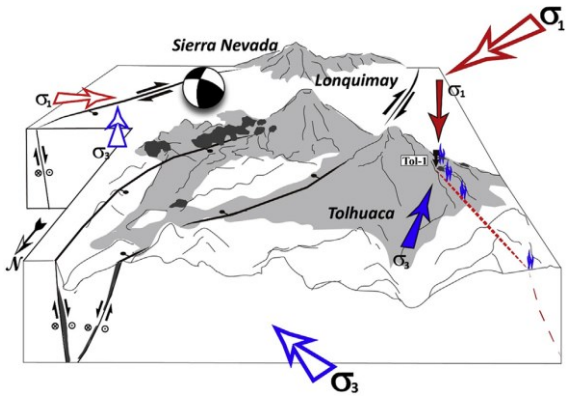

Figure 3: Schematic block diagram taken from Perez-Flores et al., (2017) illustrating the proposed tectonic setting of Tolhuaca-Lonquimay volcanoes (looking south). The model shows the spatial distribution of flank-vents (dark grey), fumaroles (blue flames), stratovolcanoes and faults, which are kinematically compatible with regional stress field (biggest unfilled arrows) (Lavenu and Cembrano, 1999; Pérez-Flores et al., 2016) and local stress field solution (filled arrows) at the Tol-1 core location.

3.6 Effects of the Clay Cap on Thermal Structure: Numerical Simulations

In order to explore the effect of the development of a low-permeability clay cap on the physical evolution of the Tolhuaca geothermal system, we performed numerical simulations of coupled heat and fluid flow using HYDROTHERM (Hayba and Ingebritsen, 1994). The modelled heat source of the system is a magma body that instantly intrudes to a depth of ~3 km beneath the volcano summit. Two scenarios were considered, namely, with and without the presence of a low-permeability clay cap. In both scenarios, the intrusion of a shallow (~ 3 km) magma body results in an increase in enthalpy of the fluid and a decrease in fluid pressures as a result of a transition from the hydrostatic pressure gradient to a liquid-saturated (boiling) environment at reservoir depths (>670 m).

The main differences caused by the presence of a low-permeability layer or clay cap can be described in temperature and vapour fraction evolution. In the absence of a clay cap, boiling conditions (maximum temperature for depth) are restricted to the deep part of the reservoir (> 1.1 km) after 10 ka, and only for a short period of time (~3 ka). In contrast, in the presence of a clay cap the reservoir heats up faster and reaches boiling conditions (flat and constant temperature) near 5 ka at shallower reservoir depths (~0.9–2 km) and vapour fractions of up to 15 vol. %. Boiling conditions are sustained for a longer period of time (~10 ka) before disappearing after 15 ka.

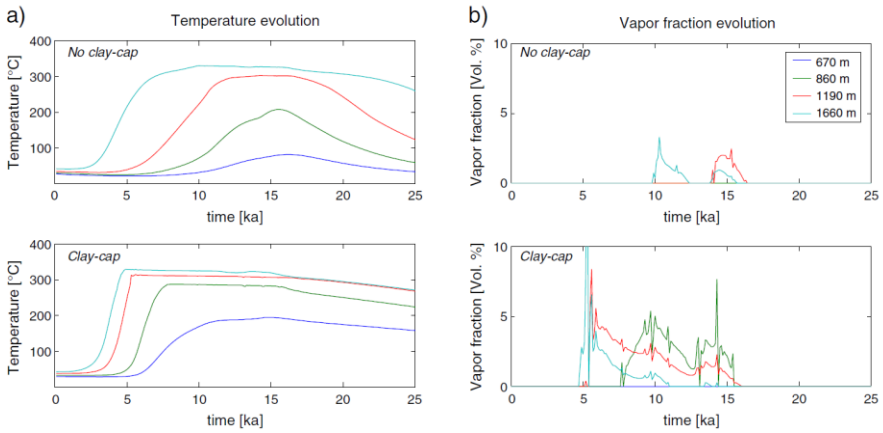

Figure 4: Evolution of temperature (ºC) and vapour (vol%) fraction as a function of time (ka) simulated for a Tolhuaca-like system under two scenarios, namely, with and without a low permeability clay cap. Four selected depths (coloured) depict the thermal structure in the vertical axis. A. Temperature evolution. The almost constant and flat temperature profile marks two-phase fluid conditions (boiling). B. Volumetric vapour fraction. Values above 0% indicate two-phase fluid conditions. Temperature and two-phase fluid conditions are maximised on the duration and vertical extension when a clay cap is present.

4. CONCLUSIONS

The evolution of hydrothermal alteration at Tolhuaca has produced a mineralogical, hydrological and structural vertical segmentation of the system through the development of a low-permeability, low-cohesion clay-rich cap at shallow depth. The quantitative chemical analyses of fluid inclusions and borehole fluids reveal a significant change in chemical conditions during the evolution of Tolhuaca. While borehole (present-day) fluids are rich in Au, B and As, but Cu-poor (B/Na ~ $10^{0.5}$, As/Na ~ $10^{-1.1}$, Cu/Na ~ $10^{-4.2}$), the paleofluids trapped in fluid inclusions are Cu-rich but poor in B and As (B/Na ~ 10^{-1}, As/Na ~ $10^{-2.5}$, Cu/Na ~ $10^{-2.5}$ in average). The clear correspondence between Cu and As concentrations between pyrite-forming fluids (present-day and paleofluids) and chemical zonation in pyrite provides direct evidence supporting the selective partitioning of metals into pyrite as a result of changes in hydrothermal fluid composition, most likely due to separation of a single-phase fluid into a low-density vapour and a denser brine, capable of fractionating Cu and As (Tardani et al., 2017).

Inversion of fault-slip data indicates a local tensional stress field with a vertically oriented σ_1 axis (083/74) and a subhorizontal, NS-trending σ_3 axis (184/03). Within the topmost 400 m of the borehole, faults and veins are randomly oriented, whereas below 400 m depth, faults and veins show preferential NE- to EW-strikes and steep (> 50°) dips. The EW-striking veins are compatible with the calculated local stress field whereas NE-striking veins are compatible with the regional stress field, the morphological elongation of volcanic centres, alignments of flank vents and dyke orientation. Furthermore, these data show that the bulk transpressional regional stress field has local variations to a tensional stress field within the NE-striking fault zone belonging to the Liquiñe-Ofqui Fault Zone, favouring the activation of both NW- and NE-striking pre-existent discontinuities, especially the latter which are favourably oriented to open under the prevailing stress field (Perez-Flores et al., 2017).

Numerical simulations of heat and fluid flow indicate that the presence of a low permeability clay cap increases the duration of liquid-saturated conditions (boiling temperatures) by a factor of three at the Tolhuaca reservoir depth (propylitic zone) and extends the lifespan of the hydrothermal system significantly (Sanchez-Alfaro et al., 2016). Simulations suggest that such an effect is mainly produced by the barrier effect that the low-permeability layer has on the cold meteoric water down-flow. As in high relief regions, the driving force for meteoric water down-flow increases, the effect of a low-permeability layer is likely to be enhanced in hydrothermal systems that develop near the flank of stratovolcanoes, compared to flat areas.

REFERENCES

Aravena D., Muñoz M., Morata D., Lahsen A., Parada M. A., Dobson P. (2016) Assessment of high enthalpy geothermal resources and promising areas of Chile. Geothermics **59**, 1–13. doi:10.1016/j.geothermics.2015.09.001.

Browne, P.R.L., 1978. Hydrothermal Alteration in Active Geothermal Fields. Annu. Rev. Earth Planet. Sci. 6, 229–248. doi:10.1146/annurev.ea.06.050178.001305

Davatzes, N.C., Hickman, S.H., 2010. The Feedback Between Stress, Faulting, and Fluid Flow: Lessons from the Coso Geothermal Field, CA, USA, in: Proceedings World Geothermal Congress 2010 Bali, Indonesia, 25-29 April 2010.

Dobson, P.F., Kneafsey, T.J., Hulen, J., Simmons, A., 2003. Porosity, permeability, and fluid flow in the Yellowstone geothermal system, Wyoming. J. Volcanol. Geotherm. Res. 123, 313–324. doi:10.1016/S0377-0273(03)00039-8

Meller, C., Kohl, T., 2014. The significance of hydrothermal alteration zones for the mechanical behavior of a geothermal reservoir. Geotherm. Energy 2, 12. doi:10.1186/s40517-014-0012-2

Melosh G., Cumming W., Benoit D., Wilmarth M., Colvin A., Winick J., Soto E., Sussman D., Urzúa-Monsalve L., Powell T., Peretz A. (2010) Exploration results and resource conceptual model of the Tolhuaca Geothermal Field, Chile, in: Proceedings World Geothermal Congress, Bali, Indonesia, 25-29 April 2010.

Melosh G., Moore J., Stacey R. (2012) Natural reservoir evolution in the Tolhuaca geothermal field, southern Chile, in: 37th Workshop on Geothermal Reservoir Engineering Stanford University, Stanford, California, January 31 - February 1, 881 2012. SGP-TR-194.

Moore, J.N., Simmons, S.F., 2013. More power from below. Science (80-.). 340, 933–4. doi:10.1126/science.1235640

Pérez-Flores, P., Cembrano, J., Sánchez-Alfaro, P., Veloso, E., Arancibia, G., Roquer, T. (2016) Tectonics, magmatism and paleo-fluid distribution in a strike-slip setting: insights from the northern termination of the Liquiñe–Ofqui Fault System, Chile. Tectonophysics **680**, 192–210.

Pérez-Flores, P., Veloso, E., Cembrano, J., Sánchez-Alfaro, P., Lizama, M., & Arancibia, G. (2017). Fracture network, fluid pathways and paleostress at the Tolhuaca geothermal field. *Journal of Structural Geology*, *96*, 134-148.

Sánchez-Alfaro P., Reich M., Arancibia G., Pérez-Flores P., Cembrano J., Driesner T., Lizama M. Rowland J., Morata D., Heinrich C. A., Tardani D., Campos E. (2016a) Physical, chemical and mineralogical evolution of the Tolhuaca geothermal system, southern Andes, Chile: insights into the interplay between hydrothermal alteration and brittle deformation. J.Volcanol. Geoth. Res. **324**, 88–104.

Sanchez-Alfaro, P., Sielfeld, G., Campen, B. Van, Dobson, P., Fuentes, V., Reed, A., Palma-Behnke, R., Morata, D., 2015. Geothermal barriers, policies and economics in Chile – Lessons for the Andes. Renew. Sustain. Energy Rev. 51, 1390–1401. doi:10.1016/j.rser.2015.07.001

Tardani, D., Reich, M., Deditius, A.P., Chryssoulis, S., Sánchez-Alfaro, P., Wrage, J., 2017. Cu-as decoupling in an active geothermal system: a link between pyrite and fluid composition. Geochim. Cosmochim. Acta 204, 179–204.